Unconstrained Biometric Recognition based on Thermal Hand Images

Ewelina Bartuzi[1,⋆], Katarzyna Roszczewska[1], Adam Czajka[2], Andrzej Pacut[3]

[1] Research and Academic Computer Network (NASK), Warsaw, Poland
[2] University of Notre Dame, IN, USA
[3] Warsaw University of Technology, Warsaw, Poland
⋆ Presenting co-author (email: ewelina.bartuzi@nask.pl)

6th IAPR/IEEE International Workshop on Biometrics and Forensics
IWBF 2018, June 7-8, Sassari, Italy

Motivation

This work proposes a biometric recognition method based on thermal images of inner part of the hand. Hand temperature is associated to pattern of blood vassels and measurement is hygienic, non-invasive, fast, independent of ambient light. Additionally, thermal information can by difficult to reconstruct with a spooth artifact.

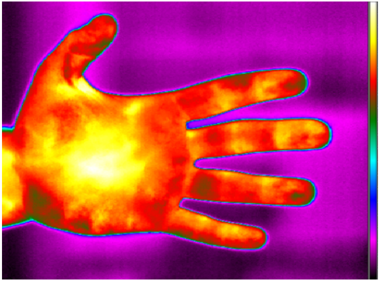

Q1. **Is the distribution of hand temperature measured by a thermal sensor in unconstrained setup unique?**

Q2. **Are the thermal features stable and able to offer a reliable biometric recognition after a period of time?**

Q3. **Which technique of feature etraction and classification applied to thermal images delivers the highes accuracy?**

Data Acquisition

1. 21, 000 thermal maps in BioBase-Hand-Thermal:

70 subjects $\times$ 3 sessions $\times$ 2 hands (left and right) $\times$ 5 presentation $\times$ 10 frames

2. Measuring device: thermal camera FLIR SC645
3. Resolution: 640×480 pixels
3. Challenge: unconstrained position of the hand
4. Measurement conditions: office environment (22^{0}C)
5. Metadata: factors affecting the hand temperature
6. Access: available for research purposes

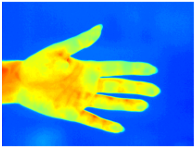
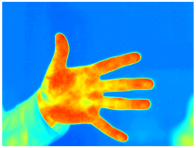
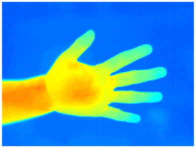
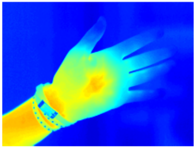

Image preprocessing stages

1. **Segmentation** ▽
   - **Otsu's method** - segmentation threshold maximizes the variance between the background class and the object, and minimalizes the intra-class variance
   - **Method based on GMM** - calculate the intersection point of two Gaussian curves, which approximate the distributions of object's values and of the background's values
2. **ROI extraction** ▼
3. **Hand alignment** ▼

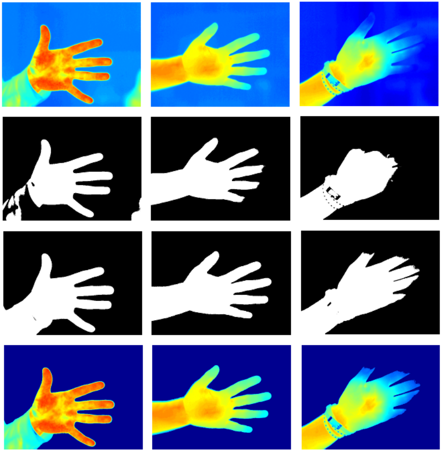

Image preprocessing stages

1. Segmentation ▼
2. **ROI extraction** ▽
   - **distance map extraction** - each element of the distance map is the Euclidean distance to the nearest point lying on the contour.
   - **finding the largest distance** - the maximum element of the distance map determines the circular ROI (position and radius)

3. Hand alignment ▼

Image preprocessing stages

1. Segmentation ▼
2. ROI extraction ▼
3. **Hand alignment** ▽

- noticeable similarity between distance maps of different subjects
- distance maps are not stable on the whole palm area
- the central part of a line representing maximum values of the Euclidean distance from the wrist region to the top of a middle finger

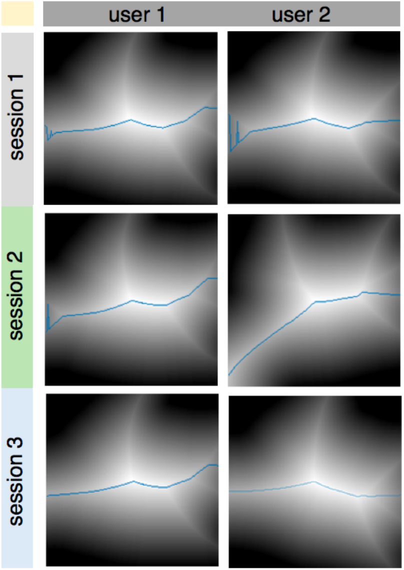

Image preprocessing stages

1. Segmentation ▼
2. ROI extraction ▼
3. **Hand alignment** ▽

- distance maps are not stable in respect to the whole palm area

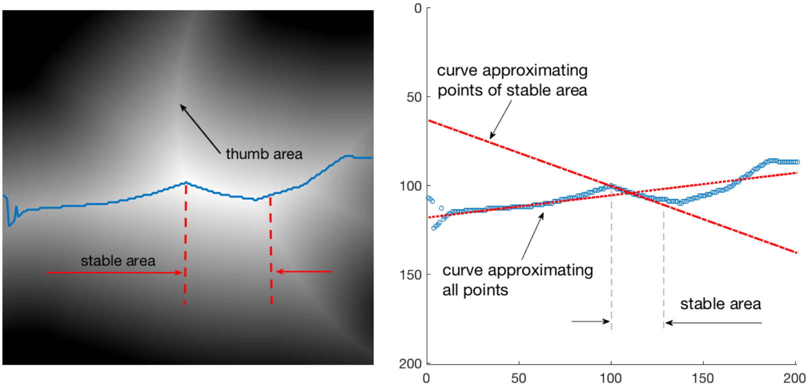

Feature extaction and classification

feature engineering approach		feature learning approach	
BSIF	Gabor filters	SimpleNet-4	VGG-16
with or without thermal stability maps			
$\chi_2 = \frac{1}{2}\sum_{i,j}\frac{(B(i,j)-B_0(i,j))^2}{B(i,j)+B_0(i,j)}$			

BSIF: Binarized Statistical Image Features

- generates a series of binary images that can be used as binary codes
- each bit of the output binary code is associated with a specific filter
- the code length is determined by number of filters in the filter bank
- 8 window sizes: from 3×3 to 17×17 pixels
- three kind of filters obtained using ICA:
  - original kernels trained on natural images *e.g.* grass, stones, fur, trees, landscapes (Huangac, 2008)
  - kernels trained on multiple patches of twenty thermal images selected randomly from the corpus collected in this work,
  - kernels trained on multiple patches of twenty images chosen randomly from a database of infrared hand vein samples (Wang, 2005).

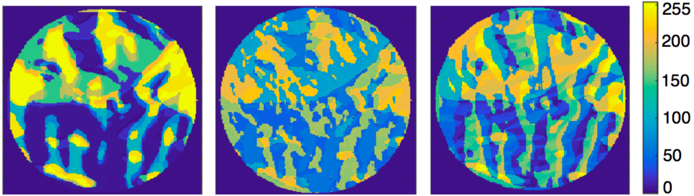

Gabor filters

- two-dimensional real-valued Gabor kernel given by:

$$f(x,y) = \frac{1}{2\pi\sigma_x\sigma_y} e^{-\left(\frac{x_\theta^2}{2\sigma_x^2} + \frac{y_\theta^2}{2\sigma_y^2}\right)} \cos\left(\frac{2\pi}{\lambda} x_\theta + \psi\right) \qquad (1)$$

$$x_\theta = x\cos\theta + y\sin\theta$$
$$y_\theta = -x\sin\theta + y\cos\theta$$

- 8 orientations: $\theta \in \{90°, 60°, 45°, 30°, 0°, -30°, -45°, -60°\}$
- 10 wavelengths: $\lambda \in \{3, 5, 7, 9, 11, 13, 15, 17, 19, 23\}$

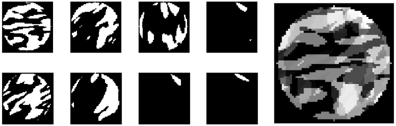

Thermal Stability Maps

- standard deviation maps of thermal data for each person
- used to calculate weight matrices for all ROI pixels: $w(x,y) = 1 - \frac{\sigma(x,y)}{\sigma_{\max}}$

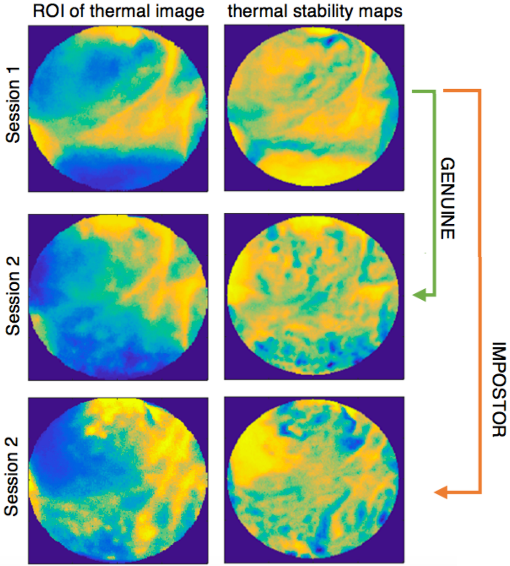

CNN-based approach

	SimpleNet-4	**VGG-16**
layers	4 convolutional layers with ReLU and max pooling 1 fully connected softmax	13 convolutional layers with ReLU and max pooling 3 fully connected softmax
sizes of filters	$13 \times 13, 9 \times 9, 7 \times 7, 5 \times 5$	3×3
no. of filters	2:32, 2:64	3, 2:64, 2:128, 3:256, 5:512
optimization	SGD, $m = 0.9$	SGD, $m = 0.9$
learning rate	$0.05 - 0.0005$	0.0001
training	on thermal images	on natural images and fine-tuned using transfer learning on thermal images
other	data augmentation	data augmentation 50% dropout

Experimental scenarios

- 10 random splits into evaluation and testing subsets
- two scenarios for template creation

	First scenario	**Second scenario**
training set	Session 1	Session 1 and Session 2
test set	Session 1, Session 2 or Session 3	Session 3
aims:	• Discriminatory information assessment • Evaluation of temporal stability	• Method evaluation after extending the reference set

Experimental results

Method	S1→ S1	S1→ S2	S1→ S3	S1+S2→ S3
BSIF (f: original)	**5.34%**	20.01%	**28.76%**	**30.24%**
BSIF (f: thermal)	8.66%	21.82%	32.79%	32.79%
BSIF (f: veins)	9.08%	**19.15%**	31.74%	31.74%
BSIF (f: original, SM)	0.90%	17.63%	**28.62%**	**27.98%**
BSIF (f: thermal, SM)	2.21%	**17.55%**	30.93%	29.85%
BSIF (f: veins, SM)	**0.36%**	17.86%	28.95%	28.95%
Gabor-based (SM)	0.28%	22.20%	32.98%	29.98%
SimpleNet	0.40%	28.80%	38.20%	36.80%
VGG-16	**0.00%**	**11.42%**	**26.44%**	**17.17%**

Tabela: Mean equal error rates from 10 random train-test splits for: BSIF filters trained with: **original** filters, **thermal** data, **vein** data, and the same BSIF filters weighted with thermal stability maps (**SM**), Gabor-based representation, and classification based on a deep convolutional networks.

Q1. Is the distribution of hand temperature measured by a thermal sensor in unconstrained setup unique and carries individual information?

- BSIF descriptor allowed to receive $ERR = 5.34\%$ for original filters.
- Employing stability maps to appropriately weigh the unstable regions to diminish their impact enabled to lower the intra-session EERs to below 1%.
- CNN-based methods also produces EER close to zero 0%, when testing data comes from the same session that was employed for building the reference templates.

Answer:

Thermal hand maps may deliver unique biometric features and have a potential to serve as a biometric identifier, but ....

Method	S1→ S1
BSIF (f: original)	**5.34%**
BSIF (f: thermal)	8.66%
BSIF (f: veins)	9.08%
BSIF (f: original, SM)	0.90%
BSIF (f: thermal, SM)	2.21%
BSIF (f: veins, SM)	**0.36%**
Gabor-based (SM)	0.28%
SimpleNet	0.40%
VGG-16	**0.00%**

Q2. Are the thermal features stable and offer a reliable biometric recognition after a period of time?

Method	S1→ S1	S1→ S2	S1→ S3	S1+S2→ S3
BSIF (f: original)	5.34%	20.01%	28.76%	30.24%
BSIF (f: original, SM)	0.90%	17.63%	28.62%	27.98%
VGG-16	0.00%	11.42%	26.44%	17.17%

- A significant drop in performance is observed when comparing data collected in different sessions.
- The correlation between the error rate and the time between sessions can be accidental. Probably, physiological changes over time and external conditions may have more impact.
- Regarding the best of analized *feature engineering* approach the lowest average EER was obtained for original BSIF kernels. CNN-based approach allowed lower EER.

Answer:
Hand thermal information as used in this study has limited temporal stability.

Q3. Which technique of feature extraction and classification applied to thermal images delivers the highest accuracy?

Method	S1→ S1	S1→ S2	S1→ S3	S1+S2→ S3
BSIF (f: original)	**5.34%**	20.01%	**28.76%**	**30.24%**
BSIF (f: veins)	9.08%	**19.15%**	31.74%	31.74%
BSIF (f: veins, SM)	**0.36%**	17.86%	28.95%	28.95%
VGG-16	**0.00%**	**11.42%**	**26.44%**	**17.17%**

- Re-training the BSIF filters with thermal and vein images does not increase the overall accuracy. Probably more important is to determine the nature of the temperature changes than to estimate the filters.
- The use of stability maps significantly improves the accuracy of the methods.
- The CNN-based approach gives better accuracy in each scenario.

Answer:

Information about the stability of thermal image areas brings the highest increase in accuracy for the methods based on texture descriptors, but employing CNNs have a potential for even higher recognition rates.

Conclusions

1. Hand heat distribution contains individual information
2. Presented modality is very dependent on external conditions and human physiological processes
3. It is important to determine the most stable areas in time (under different conditions)
4. Higher accuracy is obtained by using an approach based on convolutional neural networks
5. The collected database of thermal images will be available to interested researchers for non-commercial purposes
6. Further research: the dynamics of temperature changes and thermal images in presentation attack detection

Unconstrained Biometric Recognition based on Thermal Hand Images

Ewelina Bartuzi[1,⋆], Katarzyna Roszczewska[1], Adam Czajka[2], Andrzej Pacut[3]

[1] Research and Academic Computer Network (NASK), Warsaw, Poland
[2] University of Notre Dame, IN, USA
[3] Warsaw University of Technology, Warsaw, Poland
[⋆] Presenting co-author (email: ewelina.bartuzi@nask.pl)

6th IAPR/IEEE International Workshop on Biometrics and Forensics
IWBF 2018, June 7-8, Sassari, Italy

Hand images acquired by sensors of different wavelengths of light in biometrics

	visible light images	*near-infrared images*	*thermal images*
measuring device			
results			